A genetic variant of the sperm-specific SLO3 K^+ channel has altered pH and Ca^{2+} sensitivities

Received for publication, January 11, 2017, and in revised form, March 21, 2017 Published, Papers in Press, April 4, 2017, DOI 10.1074/jbc.M117.776013

Yanyan Geng[‡1], Juan J. Ferreira[§1], Victor Dzikunu[¶], Alice Butler[¶], Pascale Lybaert[§], Peng Yuan[‖], Karl L. Magleby[‡], Lawrence Salkoff[¶], and Celia M. Santi[§2]**

*From the Departments of [§]Obstetrics and Gynecology, [¶]Neuroscience, **Genetics, and [‖]Cell Biology and Physiology, Washington University School of Medicine, St. Louis, Missouri 63110 and the [‡]Department of Physiology and Biophysics, University of Miami Miller School of Medicine, Miami, Florida 33136*

Edited by Roger J. Colbran

To fertilize an oocyte, sperm must first undergo capacitation in which the sperm plasma membrane becomes hyperpolarized via activation of potassium (K^+) channels and resultant K^+ efflux. Sperm-specific SLO3 K^+ channels are responsible for these membrane potential changes critical for fertilization in mouse sperm, and they are only sensitive to pH_i. However, in human sperm, the major K^+ conductance is both Ca^{2+}- and pH_i-sensitive. It has been debated whether Ca^{2+}-sensitive SLO1 channels substitute for human SLO3 (hSLO3) in human sperm or whether human SLO3 channels have acquired Ca^{2+} sensitivity. Here we show that hSLO3 is rapidly evolving and reveal a natural structural variant with enhanced apparent Ca^{2+} and pH sensitivities. This variant allele (C382R) alters an amino acid side chain at a principal interface between the intramembrane-gated pore and the cytoplasmic gating ring of the channel. Because the gating ring contains sensors to intracellular factors such as pH and Ca^{2+}, the effectiveness of transduction between the gating ring and the pore domain appears to be enhanced. Our results suggest that sperm-specific genes can evolve rapidly and that natural genetic variation may have led to a SLO3 variant that differs from wild type in both pH and intracellular Ca^{2+} sensitivities. Whether this physiological variation confers differences in fertility among males remains to be established.

To fertilize an oocyte, sperm must first undergo capacitation within the female genital tract. During capacitation, the sperm plasma membrane becomes hyperpolarized as a result of activation of potassium channels and resultant K^+ efflux. In mouse sperm, the main K^+ current, known as IKSper, is activated by intracellular alkalization (1). In work to identify the channel responsible for this current, we and others examined sperm from an SLO3 knock-out mouse and found that it lacked the pH-sensitive K^+ current (2, 3). In addition, homozygous SLO3 knock-out males were infertile. Together, these data firmly established that SLO3 channels are responsible for sperm hyperpolarization in mice and are essential to the fertilization process (2, 3).

The situation in human sperm has been less clear. Like mouse sperm, human sperm become hyperpolarized during capacitation (4, 5), and the human K^+ current, referred to as hKSper, is somewhat less sensitive to intracellular pH than IKSper. However, unlike IKSper, the hKSper current is sensitive to intracellular Ca^{2+} (6, 7). Given that heterologous expression studies showed that murine SLO3 was sensitive to pH but not Ca^{2+} (8), human SLO3 was considered unlikely to be the channel responsible for hKSper. However, whereas human SLO3 was shown in heterologous expression experiments to be regulated by pH, its Ca^{2+} sensitivity was initially untested (9). SLO3 and SLO1 together with SLO2 make up a family of K^+ channels consisting of four transmembrane voltage sensor domains surrounding a central pore gate domain. These channels also contain a large cytosolic domain, the gating ring (10). This ring responds to intracellular signals and regulates the SLO channels. It is generally accepted that SLO1 channels (also known as big potassium (BK) channels) are mainly activated by voltage and intracellular calcium, whereas SLO3 channels are modulated by voltage and intracellular pH (pH_i). Given the Ca^{2+} sensitivity of hKSper, Mannowetz *et al.* (7) suggested that the K^+ channel responsible for hKSper was SLO1 rather than SLO3.

In contrast to this suggestion, Brenker *et al.* (6) heterologously expressed human SLO3 in *Xenopus* oocytes and Chinese hamster ovary cells and reported that this channel is sensitive to both Ca^{2+} and pH_i, leading them to conclude that SLO3 is indeed responsible for the hKSper current. This is an attractive possibility for evolutionary reasons. Whereas SLO1 channels are highly conserved across species and are expressed in numerous tissues (11–14), SLO3 channels are present only in mammals, are expressed only in spermatozoa (2, 3, 8, 15), and have low sequence conservation among mammalian species as we showed by comparing mouse and bovine SLO3 sequences (16). Likewise, numerous genes that mediate sexual reproduction (17–19), such as those involved in immune interactions affecting reproduction and other ion channels expressed in sperm (*e.g.* CatSper) (20), show similarly low sequence conservation between species. This low sequence conservation might

This work was supported by National Institute of Health Grants R01 HD069631 (to C. M. S.), R21 NS 088611 and R21 MH107955 (to L. S.), and R01 GM114694 (to K. L. M. and L. S.). The authors declare that they have no conflicts of interest with the contents of this article. The content is solely the responsibility of the authors and does not necessarily represent the official views of the National Institutes of Health.

[1] Both authors contributed equally to this work.

[2] To whom correspondence should be addressed: Dept. of Obstetrics and Gynecology, Washington University, School of Medicine, BJC Inst. of Health Bldg., 425 South Euclid, St. Louis, MO 63110. Tel.: 314-747-3306; E-mail: santic@wustl.edu.

predict high variation in functional properties. For example, we cloned and heterologously expressed the bovine SLO3 channel in *Xenopus* oocytes and showed that it differed from mouse SLO3 channels in several aspects, including the voltage range of activation, kinetics, and pH sensitivity (16). Thus, it seems plausible that human SLO3 could functionally diverge from its murine orthologue.

To further explore whether SLO3 may be undergoing accelerated variation in humans, we examined its sequence conservation within the Exome Aggregation Consortium, a database currently consisting of more than 64,000 individuals, and compared it with that of the *SLO1* gene. That analysis showed that *SLO3* is evolving significantly more rapidly in humans than *SLO1*, suggesting the plausibility of rapidly evolving functional properties that are conceivably relevant to sperm physiology. Additionally, we identified a conspicuous non-synonymous single nucleotide polymorphism in human SLO3 (hSLO3)[3] that maps to the site of interaction between the gating ring and the pore gate domain. Our biophysical characterization of this variant then showed that it confers heightened sensitivity to both Ca^{2+} and pH_i relative to the wild-type hSLO3 channel. Thus, this study illustrates not only how fast sperm-specific genes can evolve relative to genes that are expressed in somatic tissues but also how the natural structural variants produced in a sperm-specific protein can be relevant to functional properties salient to the fertilization process.

Results

Low conservation of SLO3 within the human species

We previously demonstrated that mouse and bovine SLO3 protein sequences are 62.1% identical. Here, we compared human and mouse SLO3 protein sequences and found that they are only 62.9% identical in striking contrast to the 98.2% identity between human and mouse SLO1 (Fig. 1). To examine conservation within humans, we compiled data from the single-nucleotide polymorphism (SNP) database of the National Center for Biotechnology Information and the Exome Aggregation Consortium. We found that the percentage of non-synonymous SNPs (which change the amino acid sequence) in the human *SLO3* gene was much higher than in the *SLO1* gene (66 *versus* 43%, respectively). Similarly, two other sperm-specific genes that we analyzed (the ion channel *CATSPER* and the Na^+/K^+-ATPase $\alpha 4$) also had higher percentages of non-synonymous SNPs (67 and 69%, respectively) than the somatically expressed genes *SLO2* and Na^+/K^+-ATPase $\alpha 1$ (44 and 40%, respectively) (Fig. 2). This natural structural variation in sperm-specific genes may provide a large library of possibilities to achieve a selective advantage in fertilization.

A SLO3 variant with an altered residue at a critical interface

Among the many *SLO3* non-synonymous (missense) SNPs reported in the SNP database, our attention was drawn to C382R, which would be expected to radically alter the properties of the amino acid side chain at an important position within the channel's structure. This SNP was validated by three independent criteria, and 125 chromosomes were found to carry the allele in the Exome Aggregation Consortium data, which contain the sequences of 60,706 people from diverse ethnic backgrounds. Indeed, the minor allele frequency of 0.00103 is actually surprisingly high for such a radical variation in structure. From the 420 missense *SLO3* variants found, there were only three other instances (P576T, R768W, and L955F) where a missense SNP has a higher validated minor allele frequency, a result that hints at positive selection pressure. Of further interest is the fact that an alignment of SLO3 with its close Ca^{2+}-dependent paralogue SLO1 shows that the Cys → Arg amino acid substitution places the Arg into SLO3 at a position where an Arg exists in SLO1. From the crystal structures of SLO1 and SLO3, we know that this position is at the interface between the intramembrane "core" of the channel and the cytoplasmic gating ring (Fig. 3). This interface (the α-B helix) may be important in transducing the effects of factors interacting with the gating ring, which may influence channel opening. Prior studies with SLO1 channels have shown that both Ca^{2+} and pH interact with the gating ring (14, 21–25) and have major effects on channel opening. These effects are most likely transduced, at least in part, through the α-B helix. The C382R variant substitutes a positively charged arginine residue in place of a cysteine, and the upward orientation of the charged side chain is likely to interact with residues of the voltage-gated pore of the channel. Thus, the position of the Cys → Arg SNP led us to a plausible hypothesis that the properties of Ca^{2+}- and pH-dependent gating of SLO3 might be altered by this natural SLO3 structural variation.

The structural variant hSLO3-C382R is more responsive to a change in intracellular pH

To investigate whether this SNP confers differences in functional properties of the channel, we incorporated the C382R mutation into the h*SLO3* cDNA (hSLO3-C382R), heterologously expressed it, and compared its properties with wild-type hSLO3 (hSLO3-WT) in *Xenopus* oocytes. Both hSLO3-WT and hSLO3-C382R were expressed with the auxiliary subunit LRRC52 (also referred to as the γ subunit) (26). The LRRC52 subunit has been shown to increase the level of hSLO3 expression in heterologous expression systems (9). We used the two-microelectrode voltage clamp technique to measure functional properties that may involve interaction between the gating ring and the intramembrane voltage sensor or pore gate domain (PGD). Fig. 4*A* shows that expression of both hSLO3-WT and hSLO3-C382R produced outward time-dependent non-inactivating K^+ currents when the oocytes were subjected to depolarizing step pulses. To test for pH_i sensitivity, we added 20 mM NH_4Cl to the extracellular bath solution to produce an increase in pH_i. It is known that the application of NH_4Cl produces a transient increase in pH_i in *Xenopus* oocytes that lasts 5–10 min and is followed by a decrease in intracellular pH (27). We measured the maximal current induced by the application of NH_4Cl (usually obtained in the first 2–3 min of our recordings) for both the hSLO3-C382R variant and hSLO3-WT. We found that NH_4Cl produced a larger incremental increase in the maximal current amplitudes in oocytes expressing hSLO3-C382R

[3] The abbreviations used are: hSLO, human SLO; PGD, pore gate domain; V_h, holding potential; nP_o, channel open probability; HEDTA, *N*-(2-hydroxyethyl)ethylnediamine-*N*,*N*′,*N*′-triacetic acid.

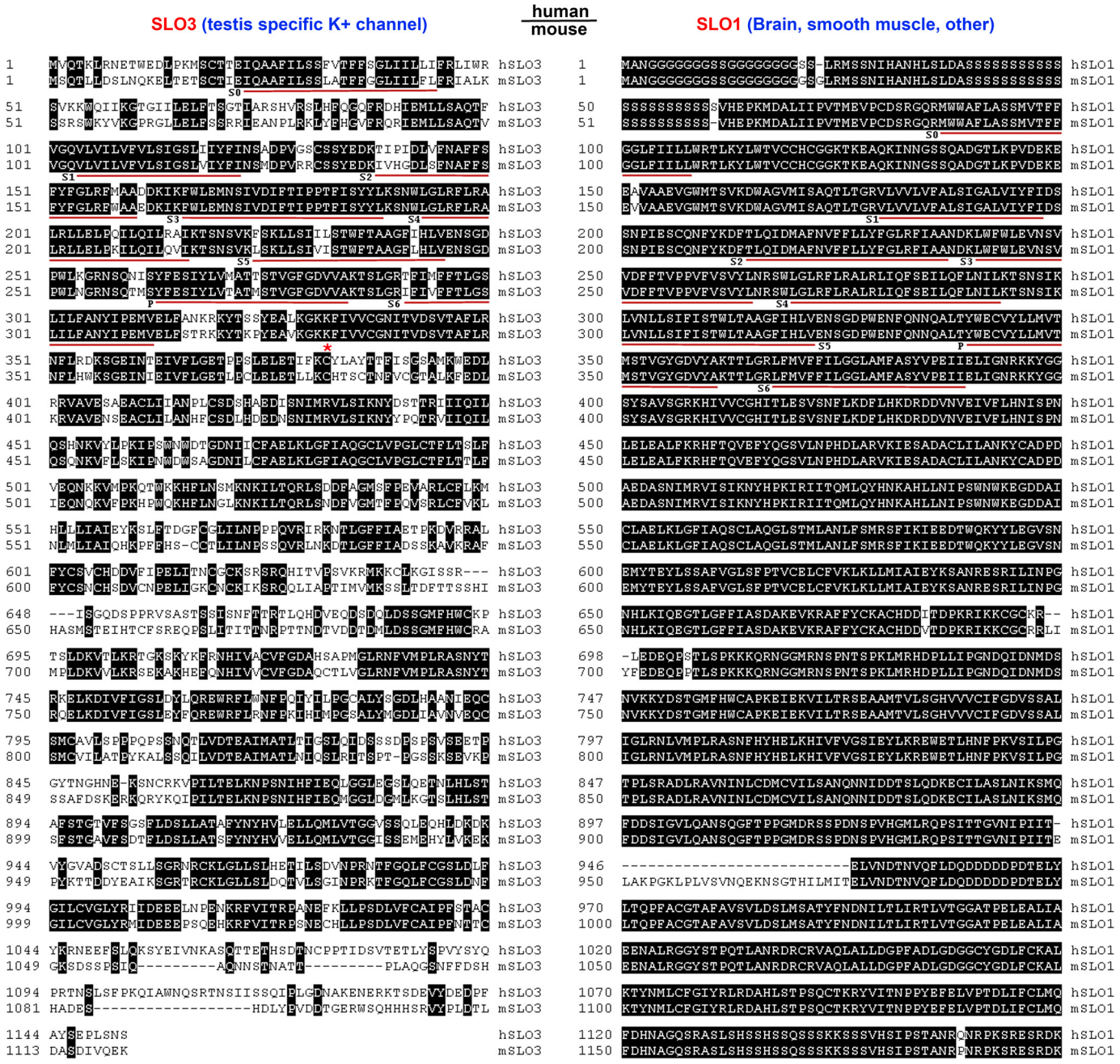

Figure 1. Interspecies (human-mouse) alignment of the amino acid sequences of SLO3 channel orthologues (*left*) compared with the interspecies (human-mouse) alignment of the amino acid sequences of SLO1 channel (*right*). Identical residues are *shaded*. SLO3 orthologues are highly divergent between human and mouse (~62.1% identity) relative to SLO1 orthologues (~98.2% identity) between the same two species, suggesting a more rapid rate of evolution. Hydrophobic segments surrounding the pore region are *underlined* with designations *S0–S6*. A *red asterisk* marks the position of the C382R variant residue.

than in those expressing hSLO3-WT (Fig. 4, *A* and *B*). Although intracellular pH is not precisely controlled in these experiments, we have found that this technique is highly reproducible and effective in demonstrating a difference in reactivity to a pH_i change as indicated by the statistics presented in Fig. 4. To further demonstrate the effect of intracellular alkalinization on channel function, we constructed conductance-voltage curves from tail currents evoked by step pulses to depolarizing potentials measured at 0 mV. These experiments showed that, under control conditions in normal saline, the activation curve of hSLO3-C382R was shifted to the right with respect to the hSLO3-WT activation curve (Fig. 4*C*). This indicates that hSLO3-C382R required more positive voltages for activation than hSLO3-WT, suggesting that the basal level of hSLO3-C382R activity was lower than that of hSLO3-WT. However, NH_4Cl caused a significantly larger leftward shift in hSLO3-C382R than in hSLO3-WT, indicating that hSLO3-C382R had a greater response to intracellular alkalinization.

Nevertheless, the final $V_{0.5}$ values achieved by hSLO3-WT and the hSLO3-C382R variant after intracellular alkalinization were similar ($V_{0.5}$ = +33 ± 2.38 mV (S.D.), n = 7 and +35.1 ± 3.0 mV (S.D.), n = 4, respectively) (Fig. 4*C*). Thus, after intra-

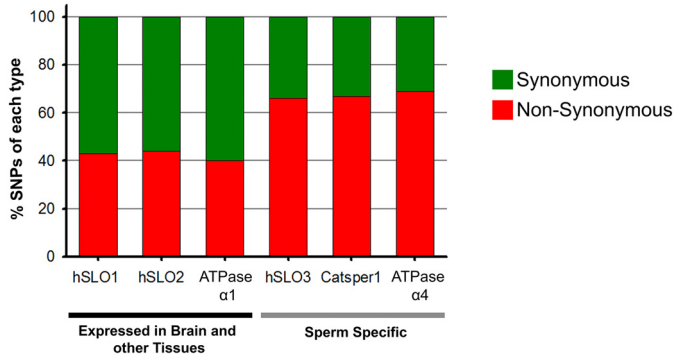

Figure 2. Rapid evolution of sperm-specific genes relative to genes expressed in brain and other tissues. The graph shows the synonymous and non-synonymous SNPs present in three sperm-specific genes relative to those present in genes expressed in brain and other tissues. SNPs that change channel structure (non-synonymous SNPs) are represented in *red*, whereas SNPs that do not (synonymous) are represented in *green*. The ratios of non-synonymous to synonymous mutations for human *SLO3 versus SLO1* gene as well as other examples given are stated in the text. The data in this graph were compiled from the NCBI SNP public database.

cellular alkalinization, the hSLO3-C382R channels end up activating in the same voltage range as the WT channels. Hence, although the greater leftward shift of hSLO3-C382R showed that this variant was more responsive to a change in pH_i than hSLO3-WT, the channel variant had significantly lower activity under basal conditions.

To confirm and amplify these findings using additional techniques, we performed inside-out patch clamp recordings. Fig. 5*B* shows that hSLO3-C382R outward currents, evoked with a step pulse protocol, were enhanced to a greater extent than hSLO3-WT currents when the cytoplasmic pH changes from 6.0 to 8.0. A voltage ramp protocol produced a similar result (Fig. 5*A*). However, Fig. 5, *A*, *B*, and *C*, also show that hSLO3-C382R had a much lower level of basal activity at low pH than hSLO3-WT (values and statistical significance are shown in Table 1). This is consistent with the result shown in Fig. 4*C* in which the conductance-voltage relation for hSLO3-C382R was shifted to more positive voltages than that for hSLO3-WT. The greater responsiveness of the hSLO3-C382R to pH_i change was largest between pH 6.0 and 7.0. Given that this is the range in which sperm capacitation occurs (28, 29), this effect is likely to be physiologically relevant.

We next used inside-out membrane patches containing a small number of channels to examine the effects of alkalinization at the single-channel level. We pulled patches from oocytes expressing hSLO3-WT or hSLO3-C382R and exposed the cytoplasmic side of the membrane to solutions with different pH values. These experiments clearly showed that, during cytoplasmic alkalinization, single-channel activity was increased to a greater degree in hSLO3-C382R than in hSLO3-WT channels (Fig. 5*C*).

From these experiments, we draw two conclusions about the effect of the variant amino acid on channel function. First, at slightly acid conditions, the activation curve of hSLO3-C382R was centered at more positive voltages than that of hSLO3-WT. This difference in the activation curves may indicate that, in the variant, the interface between the cytoplasmic gating ring and the PGD has a negative effect on intrinsic channel activity or is less effective in transducing a constitutive activating force that the gating ring applies to the gated pore. Second, hSLO3-C382R responded more sharply, with increased channel activity, than hSLO3-WT to a pH increase over the physiologically relevant intracellular pH range. Therefore it is possible that the effect of alkalinity is more efficiently transduced to the PGD at the variant interface than at the wild-type interface.

The hSLO3-C382R variant is not altered in single-channel conductance and mean open time

We next compared the single-channel properties of hSLO3-C382R and hSLO3-WT and found no differences in conductance or mean open probability. Fig. 6, *B* and *C*, show representative plots of currents, including the current-voltage (*I-V*) plot for the two channels. Mean single-channel conductances at +120 mV for hSLO3-WT and hSLO3-C382R were 71.3 ± 12.5 pS (S.D.) ($n = 14$) and 70.7 ± 7.85 pS (S.D.) ($n = 25$), respectively (symmetrical 160 mM KCl, pH_i 8). Single-hSLO3 channel conductances were slightly smaller than those reported for the mouse SLO3 channel (90 pS in asymmetrical 194 mM K^+ and 108.5 pS in 140 mM symmetrical K^+) (8, 30). However, the conductance value that we report here is very similar to previously reported values for hSLO3 (6). Mean open time values were similar for hSLO3-WT (1.57 ± 0.28 ms (S.D.), $n = 10$) and hSLO3-C382R (1.34 ± 0.38 ms (S.D.), $n = 4$) ($p = 0.24$) at pH 8.0 and 120 mV.

The hSLO3-C382R variant has increased Ca^{2+} sensitivity

Unlike mouse SLO3 channels, the activity of human SLO3 channels has been reported to be up-regulated by increases in the concentration of intracellular Ca^{2+} ($[Ca^{2+}]_i$) (6). To explore the effect of the C382R variant residue on this property, we exposed the intracellular surfaces of inside-out patches to different concentrations of Ca^{2+} and compared both macroscopic currents and single-channel currents with respect to their Ca^{2+} sensitivity. Our results confirmed the finding of Brenker *et al.* (6) that hSLO3-WT channels are calcium-sensitive (Fig. 7*B*). Also consistent with the previous report, we found that the hSLO3-WT Ca^{2+} sensitivity was orders of magnitude lower than that of SLO1 (14). However, hSLO3-C382R was sharply more responsive to increases in $[Ca^{2+}]_i$ than was hSLO3-WT. This can be seen in Fig. 7*B*, which shows macroscopic currents elicited by ramps of membrane potential from −90 to +150 mV. At +100 mV and pH 7.2, 100 μM Ca^{2+} increased the hSLO3-C382R current by ~9-fold and the hSLO3-WT current by ~4-fold (values and statistical significance are shown in Table 2). Consistent with Fig. 4, which shows that the variant channel had a positively shifted voltage range of activation, these experiments also showed that the initial level of activity before the application of Ca^{2+} was significantly lower in the variant than in the WT channel. As discussed for the experiments that examined pH_i sensitivity, this is likely because the hSLO3 variant had its activation curve shifted to a more positive voltage. This and the fact that hSLO3-C382R was more sensitive to $Ca^{2+}{}_i$ might both be explained by altered properties of transduction at the interface between the cytoplasmic gating ring and the PGD. We also noted that hSLO3-C382R showed a greater increase in Ca^{2+}-dependent current in

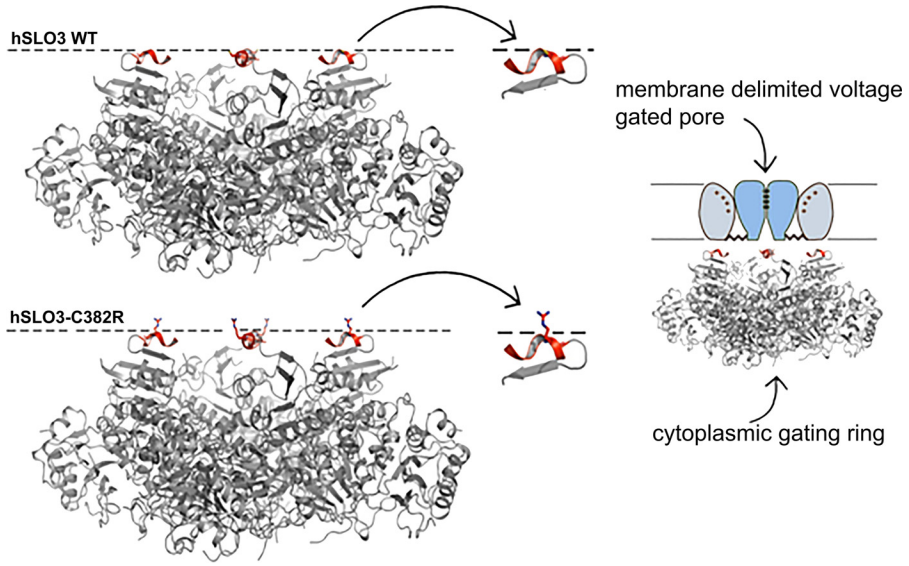

Figure 3. The C382R SNP occurs in the α-B helix of RCK1. The α-B helix is located at the transduction interface between the gating ring and the pore-gated domain. The α-B helices are colored in *red*. The C382R variant substitutes a positively charged arginine residue in place of a cysteine, and the upward orientation of the charged side chain may interact with residues of the voltage-gated pore of the channel.

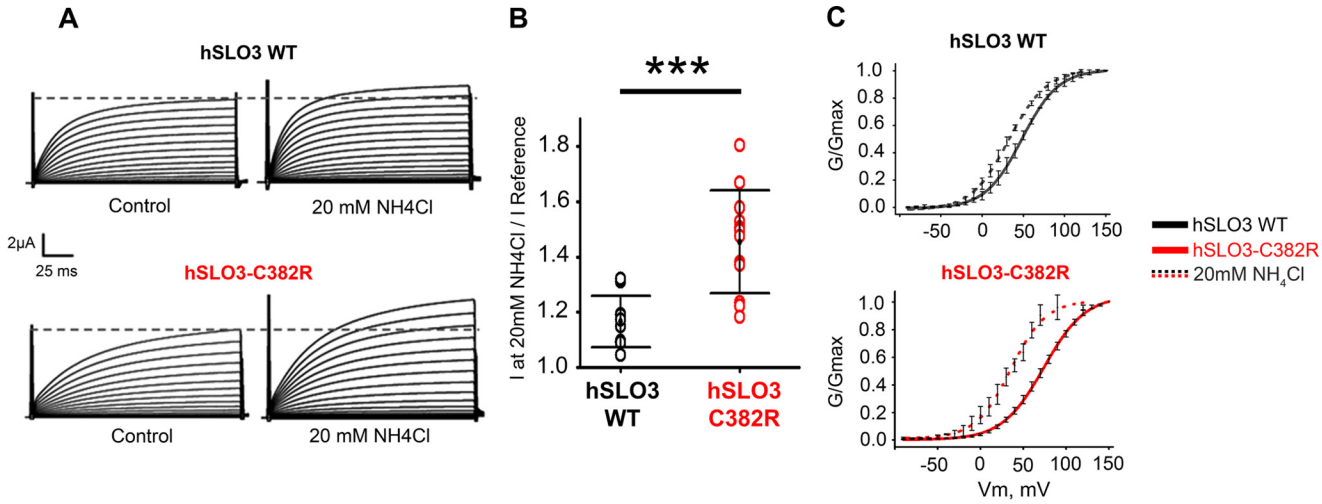

Figure 4. Effect of NH_4Cl on whole-cell outward currents of hSLO3 WT and hSLO3-C382R variant channels. *A*, whole-cell two-electrode voltage clamp recordings from hSLO3-WT- and mutant hSLO3-C382R variant-injected eggs in control conditions and in the presence of 20 mM NH_4Cl. NH_4Cl causes a larger increase in the current amplitude of hSLO3-C382R channels. In experiments using NH_4Cl, current was measured within 5 min of its application (see text). Current traces were obtained from a holding potential of −70 mV applying 10-mV steps from −90 to +150 mV. *B*, scatter plot of mean peak currents at +100 mV plotted for hSLO3-WT (*black*) and hSLO3-C382R channels (*red*). Channels were co-expressed with the γ subunit LRRC52. Mean values are as follows: hSLO3-WT, 1.17 ± 0.09 (S.D.), $n = 10$; hSLO3-C382R, 1.45 ± 0.186 (S.D.), $n = 12$. *t* tests comparing two independent groups were performed (p value <0.001). *C*, conductance *versus* voltage plots of hSLO3-WT and hSLO3-C382R. Data were obtained from tail currents at 0 mV for hSLO3-WT (*upper* plot) and for the hSLO3-C382R (*lower* plot) both in the absence and presence of 20 mM NH_4Cl. hSLO3-WT shows a $V_{0.5}$ of 48.6 ± 2.91 mV (S.D.) ($n = 53$) in control conditions and $V_{0.5}$ of 33.0 ± 2.38 mV (S.D.) ($n = 7$) in 20 mM NH_4Cl, whereas hSLO3-C382R shows a $V_{0.5}$ of 74.0 ± 1.32 (S.D.) ($n = 7$) in control conditions and $V_{0.5} = 35.0 \pm 3.0$ mV (S.D.) ($n = 4$) in 20 mM NH_4Cl. ***, $p \leq 0.001$. *Error bars* represent S.D.

the physiological range between pH 6.0 and 7.2 relative to hSLO3-WT (Fig. 7*D*).

We next examined the effect of $[Ca^{2+}]_i$ at the single-channel level (Fig. 8*B*) and found that channel open probability (nP_o) increased 2–3-fold more for hSLO3-C382R than for hSLO3-WT when $[Ca^{2+}]_i$ was increased from 0 to 100 μM at +60 mV at both pH_i 6 and 7 (Fig. 8*C*) (values and statistical significance for figure 8C are shown in Table 3). We observed insignificant differences in calcium activation at pH_i 8 ostensibly because the channel is closer to its maximum nP_o at pH_i 8 than at a lower pH_i (Fig. 8, *C* and *D*). Thus, both macroscopic and single-channel recordings showed that the hSLO3-C382R was more sharply responsive to intracellular Ca^{2+} and pH than the hSLO3-WT channel.

Finally, we examined how the pH_i sensitivity of the channels was affected by $[Ca^{2+}]_i$ and found that it was 3-fold higher in the presence of 100 μM $[Ca^{2+}]_i$ than in 0 $[Ca^{2+}]_i$ for both hSLO3-WT and hSLO3-C382R (Fig. 8*E*). We conclude that higher levels of intracellular calcium increase the response to an increase in pH_i for both hSLO3-WT and hSLO3-C382R channels.

Discussion

Because the properties of Ca^{2+}- and pH-dependent gating of SLO3 channels may be central to sperm physiology and have

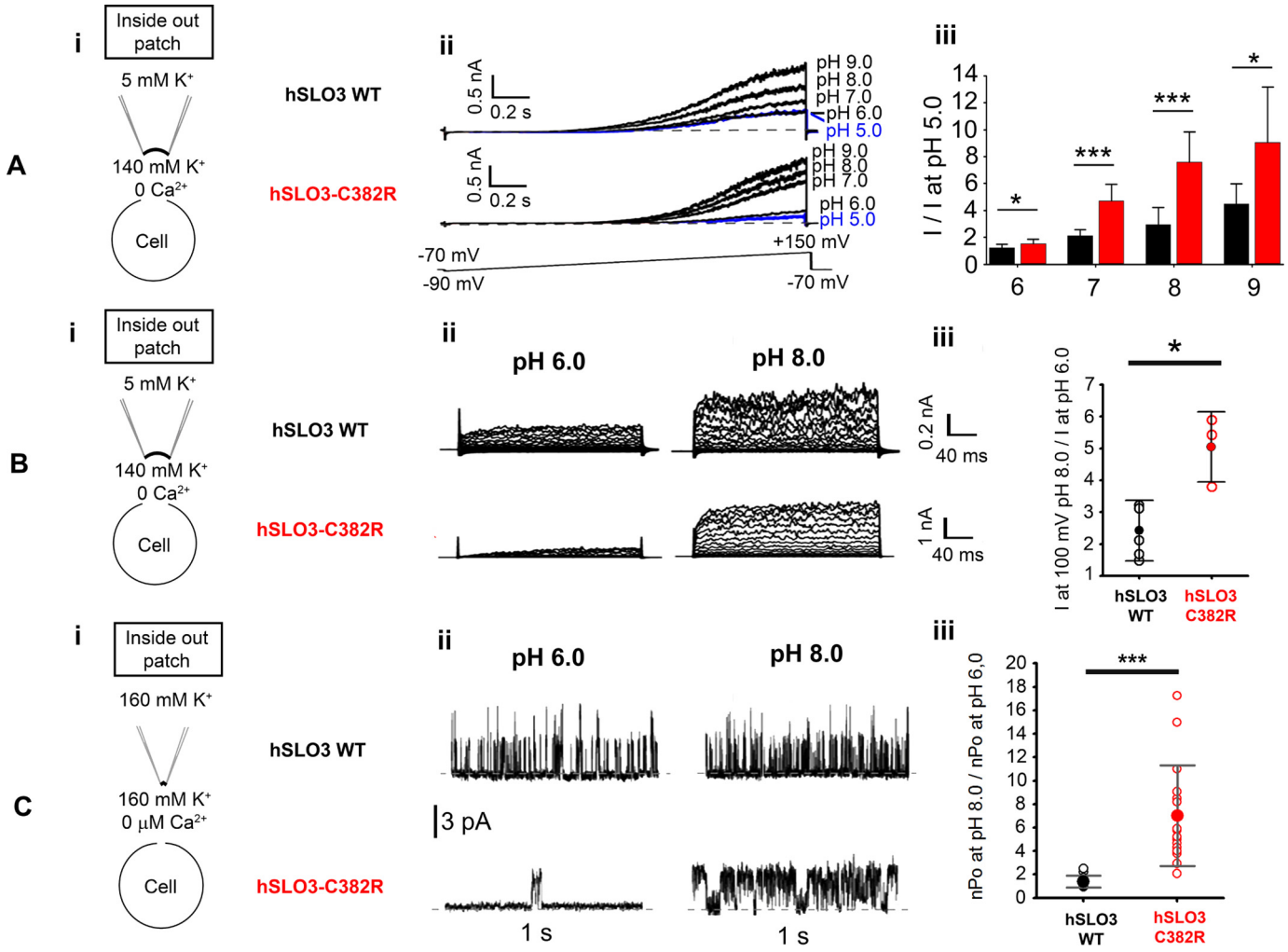

Figure 5. hSLO3-C382R channels are more sensitive to pH_i than hSLO3-WT channels. *A*, *panel i*, patch clamp (inside-out macropatch) diagram. *Panel ii*, hSLO3-WT and hSLO3-C382R currents at different intracellular pH values (5–9). Currents were obtained from a V_h of −70 mV with a ramp protocol from −90 to +150 mV in the following asymmetrical K^+ solutions: external (pipette), 135 mM $NaMeSO_3$, 5 mM $KMeSO_3$, 2 mM $MgCl_2$,10 mM Hepes, 10 mM MES, pH 7.2; internal (bath), 140 mM $KMeSO_3$, 10 mM Hepes, 10 mM MES, 1 mM EGTA (0 Ca^{2+}). *Panel iii*, normalized current values and statistics are shown in Table 1 at the indicated pH_i for WT (*black*) and C382R variant (*red*). *t* tests comparing hSLO3-WT and hSLO3-C382R were performed at each pH; *p* values at pH 6, 7, 8, and 9 are 0.024, <0.001, <0.001, and 0.027, respectively. *B*, *panel i*, patch clamp (diagram represents inside-out macropatch configuration). *Panel ii*, representative inside-out macropatch recordings from hSLO3-WT and hSLO3-C382R at different intracellular pH_i values (6 and 8). Currents were obtained from a V_h of −70 mV applying 10-mV steps from −90 to + 150 mV in the following asymmetrical K^+ solutions: external solution (pipette) 135 mM $NaMeSO_3$, 5 mM $KMeSO_3$, 2 mM $MgCl_2$,10 mM Hepes, 10 mM MES, pH 7.2; internal solution (bath), 140 mM $KMeSO_3$, 10 mM Hepes, 10 mM MES, and 1 mM EGTA (0 Ca^{2+}). *Panel iii*, graph showing relative increases of currents obtained when switching from pH 6 to 8 (at 100 mV) for hSLO3-WT and hSLO3-C382R variant. Mean values are 2.41 ± 0.948-fold (S.D.) ($n = 5$) for hSLO3-WT and 5.03 ± 0.636-fold (S.D.) ($n = 3$) for hSLO3-C382R. A paired *t* test was performed; $p = 0.012$. *C*, *panel i*, patch clamp (inside-out) diagram. *Panel ii*, hSLO3-WT and hSLO3-C382R single-channel currents at pH_i 6 and 8 obtained at +60 mV. *Panel iii*, graph showing increases in the nP_o between pH_i 6 and 8. Average nP_o increases 1.43 ± 0.518-fold (S.D.) ($n = 11$) for WT hSLO3 and 7.04 ± 4.292-fold (S.D.) ($n = 16$) for hSLO3-C382R. The following symmetrical K^+ solutions were used: external (pipette), 160 mM $KMeSO_3$, 2 mM $MgCl_2$,10 mM Hepes, 10 mM MES, pH 7.2; internal (bath), 160 mM $KMeSO_3$, 10 mM Hepes, 10 mM MES, 1 mM EGTA (0 Ca^{2+}). In all the experiments, the channels were co-expressed with the γ subunit LRRC52. *, $p \leq 0.05$; ***, $p \leq 0.001$. *Error bars* represent S.D.

Table 1

Relative pH_i sensitivity of hSLO3-WT and hSLO3-C382R

Values were obtained from inside-out macro patches at +100 mV during ramp protocols from −90 to +150 mV with a V_h of −70 mV in asymmetrical K^+ solutions at different pH_i values (6–9). Current amplitudes were normalized to the amplitude at pH 5.0. *t* tests comparing hSLO3-WT and hSLO3-C382R were performed at each pH_i. The graph and representative currents are shown in Fig. 5*A*.

pH	hSLO3	Mean	S.D.	*n*	*p* value
6.0	WT	1.24	0.26	21	0.024
6.0	C382R	1.51	0.33	9	0.024
7.0	WT	2.14	0.42	9	<0.001
7.0	C382R	4.69	1.25	5	<0.001
8.0	WT	2.94	1.29	13	<0.001
8.0	C382R	7.59	2.25	4	<0.001
9.0	WT	4.48	1.50	9	0.027
9.0	C382R	9.05	4.12	17	0.027

recently been in dispute, our findings that the hSLO3-C382R variant confers alterations to both of these functional properties bears directly on the possibility of rapid evolution and further variation of these properties in human sperm. The observation that the hSLO3-C382R variant is present in the human population at a relatively high frequency compared with most non-synonymous SNPs further hints at the possibility of positive selection for these properties. Regarding channel structure, the results also support the hypothesis that pH_i and Ca^{2+} are interacting with the gating ring of SLO3 and that the effects of those interactions are transduced to the PGD of the channel through the α-B helix.

Proteins specifically found in mammalian sperm are evolving very rapidly compared with most somatically expressed paral-

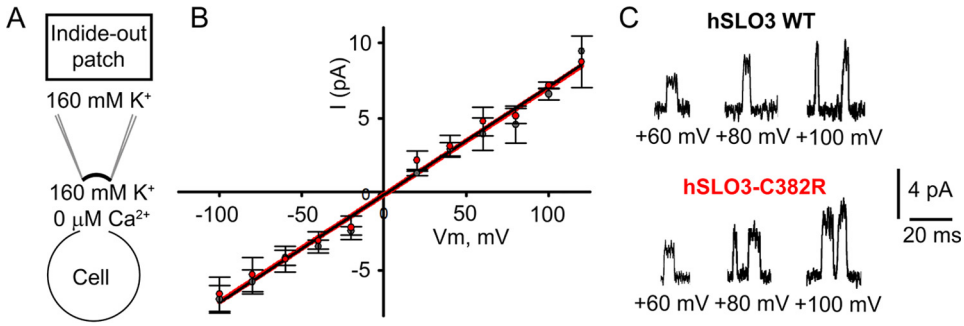

Figure 6. The hSLO3-C328R variant has no effect on single-channel conductance. *A*, patch clamp (inside-out) diagram. *B*, plot of single-channel current amplitude *versus* membrane potential. Data were obtained in the following symmetrical K^+ solutions: external (pipette), 160 mM $KMeSO_3$, 2 mM $MgCl_2$, 10 mM Hepes, 10 mM MES, pH 8.0; internal (bath), 160 mM $KMeSO_3$, 10 mM Hepes, 10 mM MES, 1 mM EGTA (0 Ca^{2+}), pH 8.0. Data are mean ± S.D. of 14 and 25 different patches for hSLO3-WT and hSLO3-C382R variant, respectively. *C*, single-channel recordings of hSLO3-WT and hSLO3-C382 channels at the indicated voltages. The mean single-channel conductance values at +120 mV were 71.3 ± 12.5 pS (S.D.) and 70.7 ± 7.85 pS (S.D.) for hSLO3-WT and hSLO3-C382R, respectively. The difference in conductance was not significant for any of the examined voltages with *p* values from 0.30 to 0.92 (*t* test). At pH 6.0 and +120 mV, the single-channel conductance was ~16% less than that at pH 8.0 for both hSLO3-WT and hSLO3-C382R, presumably due to proton block (not shown). *Error bars* represent S.D.

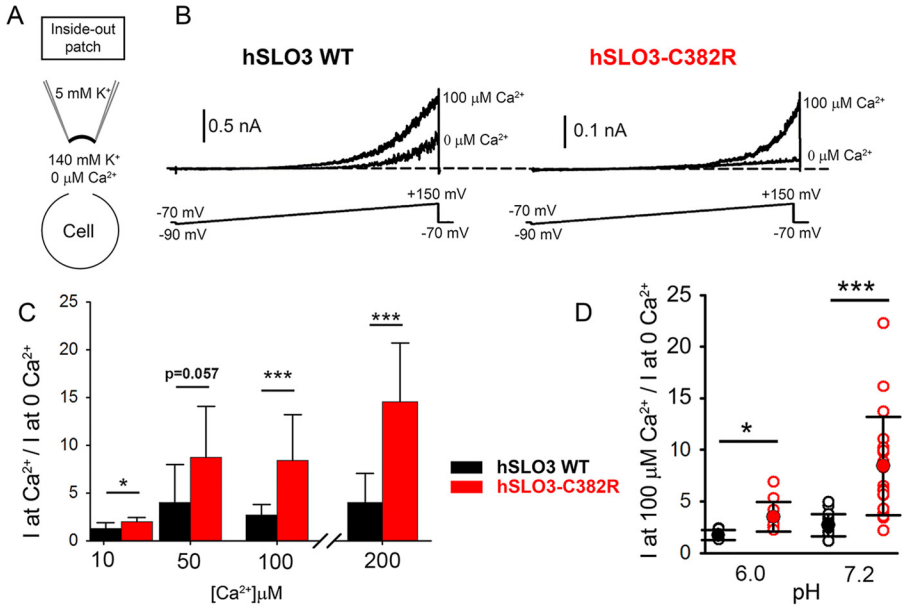

Figure 7. hSLO3-C382R is more sensitive to $[Ca^{2+}]_i$ than hSLO3 WT. *A*, patch clamp (inside-out) diagram. *B*, inside-out macropatch currents from hSLO3-WT and hSLO3-C382R variant. Records were obtained with a ramp protocol from −90 to +150 mV with a V_h of −70 mV. *C*, ratios of current amplitudes between the amplitudes of the currents recorded at the indicated $[Ca^{2+}]_i$ and 0 Ca^{2+}. See Table 2 for values and statistics. *t* tests comparing hSLO3-WT and hSLO3-C382R were performed at each $[Ca^{2+}]_i$. *p* values at 10, 50, 100, and 200 μM Ca^{2+} are 0.021, 0.057, <0.001, and <0.001, respectively. *D*, effect of pH_i on Ca^{2+} sensitivity. Ratios of current amplitudes recorded at 100 μM/0 Ca^{2+} at the indicated pH_i. Values at pH 6.0 are 1.79 ± 0.46 (S.D.) ($n = 6$) and 3.54 ± 1.43 (S.D.) ($n = 11$) for hSLO3-WT and hSLO3-C382R, respectively. Values at pH 7.2 are 2.74 ± 1.07 (S.D.) ($n = 16$) and 8.44 ± 4.75 (S.D.) ($n = 23$) for hSLO3-WT and hSLO3-C382R, respectively. *t* tests comparing hSLO3-WT and hSLO3-C382R were performed at each pH_i. *p* values at pH 6.0 and 7.2 are 0.012 and <0.001, respectively. Values for both graphs were obtained at +100 mV in the following asymmetrical K^+ solutions: external (pipette) solution, 135 mM $NaMeSO_3$, 5 mM $KMeSO_3$, 2 mM $MgCl_2$,10 mM Hepes, 10 mM MES, pH 7.2; internal (bath), 140 mM $KMeSO_3$, 10 mM Hepes, 10 mM MES, 1 mM EGTA (0 Ca^{2+}).*, $p \leq 0.05$; ***, $p \leq 0.001$. *Error bars* represent S.D.

ogues from mouse and humans (16, 31). This has been hypothesized to be due to positive Darwinian selection acting on many sperm components. One possible explanation for the high rate of variation in sperm-specific genes is that, given sperm competition between males, the rapid divergence of sperm-specific proteins favors the probability of successful fertilization (18). The sperm-specific potassium channel SLO3 with its high percentage of non-synonymous genomic SNPs seems typical of this small and special class of proteins. The physiological role of SLO3 channels in the mouse was elucidated as a result of the use of the SLO3 knock-out mice (2, 3, 32, 33). Although the role of SLO3 in the mouse is relatively well established, the situation is less clear in human sperm. First, a Ca^{2+}- and pH_i-activated K^+ current was recorded in human (7). Since the publication of this first study, heterologous expression of hSLO3 channels was used to show that hSLO3-WT channels have a sparing but measurable Ca^{2+} sensitivity (6). Here, we report that the naturally occurring variant hSLO3-C382R is significantly more sensitive than the hSLO3-WT channels to both pH_i and Ca^{2+}. However, these results do not eliminate the possibility that the hSLO1 channel in some way also participates in the hKSper current either independently or as a heteromultimeric channel in combination with hSLO3 and the γ subunit.

SLO3 channels are highly homologous to SLO1 (big potassium (BK)) channels, especially in the transmembrane regions, with most of the differences located in the cytoplasmic N- and

Table 2
Ca^{2+} sensitivity for hSLO3-WT and hSLO3-C382R

Experiments were obtained from inside-out macro patches at +100 mV during ramp protocols from −90 to +150 mV with a V_h of −70 mV and at different $[Ca^{2+}]_i$ values. Experiments were done in asymmetrical K^+ solutions. Mean values indicate the ratio between amplitude current at the specified $[Ca^{2+}]$ and 0 Ca^{2+}. All recordings were obtained at pH_i 7.2. *t* tests comparing hSLO3-WT and hSLO3-C382R were performed at each Ca^{2+} concentration. The graph and representative records of data are shown in Fig. 7.

$[Ca^{2+}]$	hSLO3	Mean	S.D.	*n*	*p* value
μM					
10	WT	1.32	0.60	6	0.021
10	C382R	2.02	0.44	9	0.021
50	WT	4.05	3.91	8	0.057
50	C382R	8.76	5.29	9	0.057
100	WT	2.74	1.07	16	<0.001
100	C382R	8.44	4.75	23	<0.001
200	WT	4.02	3.03	8	<0.001
200	C382R	14.57	6.14	8	<0.001

C-terminal regions. The SLO family channels are composed of four transmembrane voltage sensor domains surrounding a central PGD and a large cytosolic domain known as the gating ring (10). The gating ring is assembled from the regulators of K^+ conductance (RCK1 and RCK2) domains of each of the four subunits (9, 34), forming a ring with a central opening. The gating rings regulate SLO channels in response to intracellular signals. For example, removing the gating ring in SLO1 channels removes all Ca^{2+} and Mg^{2+} sensitivity, converting the SLO1 channel into a purely voltage-sensitive channel (25). In mouse SLO3, the gating ring seems to confer pH_i sensitivity, but the precise site of pH_i modulation has not been determined. Swapping the gating rings between SLO1 and SLO3 alters the channels' sensitivities to Ca^{2+} and pH_i (35). However, the gating ring structure is similar between SLO1 and SLO3 channels, especially in the critical RCK1 region (N-lobe layer), which determines the closed *versus* open conformational state of the gating ring (9) and transduces the effects of any factor interacting with the gating ring to the PGD.

The C382R variant that we identified is located in the α-B helix of the N-lobe in RCK1. Given its location and the orientation of the side chain at the interface between the gating ring and PGD, this variant likely affects the properties of the channel by affecting transduction of forces between the gating ring and the PGD rather than by altering the affinity of a calcium ion-binding site or pH-interacting site. This hypothesis is supported by our observation that hSLO3-C382R was more sensitive to changes in both pH_i and $[Ca^{2+}]_i$ than hSLO3-WT. Notably, in hSLO3-C382R, the biggest change in channel activity took place between pH_i 6 and 7, which corresponds to the intracellular pH values reported for human sperm of pH 6.8–7.0 (29). During capacitation, pH_i increases by ~0.2 unit (28, 36); under these conditions, hSLO-C382R will show a much larger increase in channel activity than hSLO3-WT. Additionally, we found that high intracellular calcium concentrations increased the pH_i sensitivity (between pH 6 and 8) of both hSLO3-WT and hSLO3-C382R channels, raising the possibility that when intracellular calcium levels increase (for example during capacitation) the SLO3 channels will become more active. In conclusion, natural genetic variation appears to have created a channel form variant that differs in activation from wild type with respect to two key factors involved in sperm physiology: pH_i and intracellular Ca^{2+} concentration. It remains to be determined whether such differences confer differences in fertility among males.

Experimental procedures

It is the policy of Washington University that all procedures using animals must be reviewed and approved by the Animals Studies Committee of Washington University (St. Louis, MO) and must be performed in accord with the National Institutes of Health Guide for the Care and Use of Laboratory Animals. However, no animals were used in these studies. *Xenopus* oocytes were purchased from Ecocyte Biosciences, Austin, TX.

The h*SLO3*-WT channel cDNA (*KCNU1*, NCBI GeneID 157074213) was obtained from Dr. Roderick MacKinnon at The Rockefeller University (9). The human *LLRC52* cDNA was obtained from Dr. Chris Lingle at Washington University (37). Channel protein sequences in Fig. 1 are human SLO3 (9), mouse SLO3 (8), human SLO1 (38), and mouse SLO1 (13). The hSLO3-C382R variant construct was synthesized by overlap extension PCR and standard cloning techniques.

For expression of channel proteins in *Xenopus* oocytes, we followed the protocol of Schreiber *et al.* (8). Briefly, the entire open reading frame with an added Kozak initiator sequence was subcloned into the pOocyte-Xpress vector, and cRNAs were produced with the mMessage mMachine (Ambion) as described previously (39).

To examine conservation within humans, we compiled data from the SNP database of the National Center for Biotechnology Information and the Exome Aggregation Consortium. The structural models presented in Fig. 3 of the gating rings for hSLO3-WT and hSLO3-C382R were based on the crystal structure published previously (9).

Expression of hSLO3-WT and hSLO3-C382R channels in Xenopus oocytes

Oocytes were harvested from female *Xenopus laevis* as described in Yuan *et al.* (40). Defolliculated oocytes were injected with 46 ng of cRNAs from hSLO3-WT and hSLO3-C382R using a Drummond Scientific nanoinjector (Broomall, PA). These cRNAs were co-injected with cRNA encoding the human LRRC52 subunit at a 1:1 ratio by mass. Injected oocytes were kept at 18 °C in ND96 medium. ND96 medium contains 96 mM NaCl, 2 mM KCl, 1.8 mM $CaCl_2$, 1 mM $MgCl_2$, 5 Hepes, pH 7.5 (with NaOH). Channel expression was tested in oocytes 3–5 days after injection with the two-electrode voltage clamp recording technique as described previously (39).

Electrophysiology experiments in Xenopus oocytes

Whole-cell current recordings from *Xenopus* oocytes were performed while the oocytes were perfused with ND96 medium + 2 μM 4,4′-diisothiocyanatostilbene-2,2′-disulfonic acid to block endogenous chloride currents (catalogue number D3514, Sigma-Aldrich). All recordings were obtained using voltage protocols specified in each figure. For patch clamp experiments, the vitelline membrane of the oocytes was mechanically removed. For patch clamp pipettes, borosilicate glass capillaries with an inner diameter of 0.86 mm, outer diameter of 1.2 mm, and length of 152 mm were obtained from World Precision

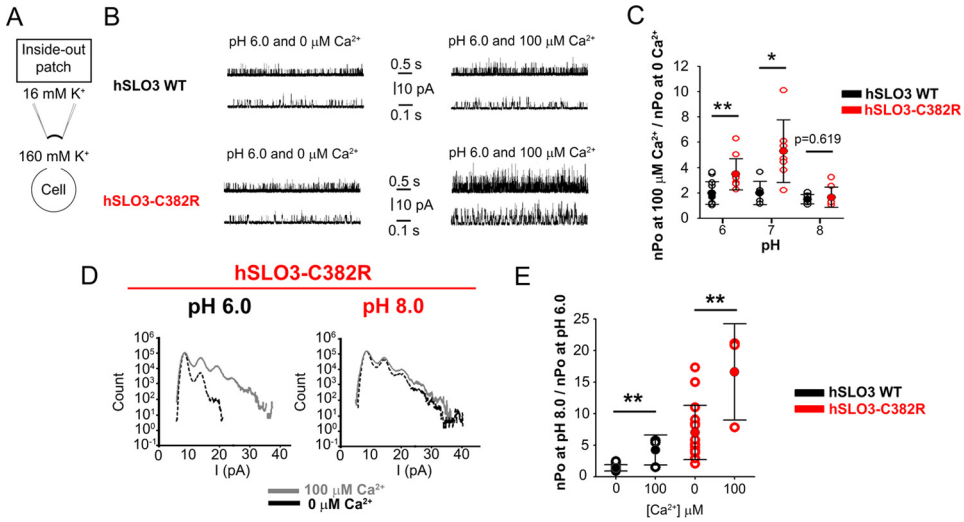

Figure 8. Single-channel currents from hSLO3 WT and hSLO3-C382R variant at different $[Ca^{2+}]_i$. *A*, patch clamp (inside-out) diagram. *B*, representative single-channel recordings of hSLO3-WT and hSLO3-C382R variant at 0 and 100 μM $[Ca^{2+}]_i$ acquired at +60 mV. Traces are shown on two different time scales. Single-channel recordings were made in asymmetrical K^+ with 160 mM KCl in the bath solution and 16 mM KCl in the pipette. The increase in nP_o for the hSLO3-C382R variant was approximately 2–3-fold greater than that seen in WT for increases in $[Ca^{2+}]_i$ from 0 to 100 μM at +60 mV. The following solutions were used in *B* and *D*: 160 mM KCl, 10 mM MES, 5 mM HEDTA in the bath solution for 0 Ca^{2+} solutions and 160 mM KCl, 2 mM $MgCl_2$, 10 mM MES, pH 7.0, in the pipette. *C*, graph showing ratios between nP_o at 100 μM Ca^{2+} and 0 Ca^{2+} at different pH_i. See Table 3 for values and statistics. *t* tests comparing hSLO3-WT and hSLO3-C382R were performed at each pH_i. *p* values at pH 6, 7, and 8 are 0.002, 0.011, and 0.619, respectively. Values were obtained at +60 mV in the following asymmetrical K^+ solutions: external (pipette) 135 mM $NaMeSO_3$, 5 mM $KMeSO_3$, 2 mM $MgCl_2$,10 mM Hepes, 10 mM MES, pH 7.2; internal (bath), 140 mM $KMeSO_3$, 10 mM Hepes, 10 mM MES, 1 mM EGTA (0 Ca^{2+}). *D*, histograms of single-channel current recordings (amplitude *versus* number of samples at that amplitude) normalized to the closed channel current level (the first peak) recorded in 100 μM Ca^{2+} at pH_i 6 or 8. *E*, hSLO3-WT and hSLO3-C382R are both more sensitive to pH_i in the presence of 100 μM Ca^{2+}. The response to pH 8.0 in 100 μM Ca^{2+} is ~3-fold larger compared with the data obtained in 0 Ca^2 for both WT and hSLO3-C382R channels. Data were obtained from single-channel recordings. The values for hSLO3-WT are 1.43 ± 0.52 (S.D.) (n = 11) and 4.25 ± 2.37 (S.D.) (n = 3) at 0 and 100 μM Ca^{2+}, respectively, and for hSLO3-C382R are 7.04 ± 4.29 (S.D.) (n = 16) at 0 Ca^{2+} and 16.62 ± 7.62 (S.D.) (n = 3) at 100 μM Ca^{2+}. *t* tests comparing the two $[Ca^{2+}]_i$ were performed for each type of channel. *p* values for hSLO3-WT and hSLO3-C382R are 0.002 and 0.006, respectively. *, $p \leq 0.05$; **, $p \leq 0.01$. *Error bars* represent S.D.

Table 3

Relative Ca^{2+} sensitivity of hSLO3-WT and hSLO3-C382R single-channel recordings

Experiments were obtained from inside-out patches at +60 mV in asymmetrical K^+ solutions at different pH_i values (6–8). Values indicate the ratios between channel open probability (nP_o) at 100 μM Ca^{2+} and 0 Ca^{2+} at different pH_i values. *t* tests comparing hSLO3-WT and hSLO3-C382R were performed at each pH_i. The graph of data is shown in Fig. 8*C*.

pH	hSLO3	Mean	S.D.	*n*	*p* value
6.0	WT	1.98	0.89	14	0.002
6.0	C382R	3.47	1.24	10	0.002
7.0	WT	1.97	1.13	6	0.009
7.0	C382R	5.20	2.26	7	0.009
8.0	WT	1.50	0.38	10	0.619
8.0	C382R	1.64	0.80	8	0.619

Instruments Inc. (Sarasota, FL). The tip resistance of fire-polished pipettes ranged from 1 to 3 megohms for macropatch recordings and from 2 to 6 megohms for single-channel recordings. The voltage protocols were applied with an Axopatch 200B amplifier (Molecular Devices, Palo Alto, CA). The data were acquired with a Digidata 1440 (Molecular Devices), digitized at 10 kHz and filtered at 2 kHz (four-pole Bessel filter) for macrocurrent recordings, and digitized at 10–100 KHz and filtered at 2–10 kHz for single-channels recordings. The data were analyzed by pClamp 10.6 (Molecular Devices) and SigmaPlot 12 (Jandel Scientific, Corte Madera, CA). The conductance-voltage (*G-V*) relationships for the hSLO3-WT and hSLO3-C382R channels were obtained from two-electrode voltage clamp records of tail currents recorded at 0 mV and fitted with a Boltzmann equation. For inside-out patch experiments, solutions were applied directly to patches with a perfusion system with six to eight independent solution lines with the capacity to exchange solutions in less than 5–10 s. The solutions used in the different types of experiments are indicated in each figure legend. All experiments were performed at room temperature (22–25 °C). Most chemicals were obtained from Sigma-Aldrich.

Author contributions—C. M. S., L. S., and K. L. M. contributed to the design and supervision of experiments, analysis of data, and writing of the paper. J. J. F. carried out experiments and data analysis and helped with the writing of the manuscript. P. L., A. B., and V. D. carried out experiments. Y. G. and P. Y. carried out experiments, analyzed data, made figures, and made suggestions on the manuscript.

Acknowledgment—We thank Deborah Frank for aid in the review and preparation of the manuscript.

References

1. Navarro, B., Kirichok, Y., and Clapham, D. E. (2007) KSper, a pH-sensitive K^+ current that controls sperm membrane potential. *Proc. Natl. Acad. Sci. U.S.A.* **104,** 7688–7692
2. Santi, C. M., Martínez-López, P., de la Vega-Beltrán, J. L., Butler, A., Alisio, A., Darszon, A., and Salkoff, L. (2010) The SLO3 sperm-specific potassium channel plays a vital role in male fertility. *FEBS Lett.* **584,** 1041–1046
3. Zeng, X. H., Yang, C., Kim, S. T., Lingle, C. J., and Xia, X. M. (2011) Deletion of the *Slo3* gene abolishes alkalization-activated K^+ current in mouse spermatozoa. *Proc. Natl. Acad. Sci. U.S.A.* **108,** 5879–5884
4. Brewis, I. A., Morton, I. E., Mohammad, S. N., Browes, C. E., and Moore, H. D. (2000) Measurement of intracellular calcium concentration and

plasma membrane potential in human spermatozoa using flow cytometry. *J. Androl.* **21,** 238–249
5. López-González, I., Torres-Rodríguez, P., Sánchez-Carranza, O., Solís-López, A., Santi, C. M., Darszon, A., and Treviño, C. L. (2014) Membrane hyperpolarization during human sperm capacitation. *Mol. Hum. Reprod.* **20,** 619–629
6. Brenker, C., Zhou, Y., Müller, A., Echeverry, F. A., Trötschel, C., Poetsch, A., Xia, X. M., Bönigk, W., Lingle, C. J., Kaupp, U. B., and Strünker, T. (2014) The Ca^{2+}-activated K^+ current of human sperm is mediated by Slo3. *eLife* **3,** e01438
7. Mannowetz, N., Naidoo, N. M., Choo, S. A., Smith, J. F., and Lishko, P. V. (2013) Slo1 is the principal potassium channel of human spermatozoa. *eLife* **2,** e01009
8. Schreiber, M., Wei, A., Yuan, A., Gaut, J., Saito, M., and Salkoff, L. (1998) Slo3, a novel pH-sensitive K^+ channel from mammalian spermatocytes. *J. Biol. Chem.* **273,** 3509–3516
9. Leonetti, M. D., Yuan, P., Hsiung, Y., and Mackinnon, R. (2012) Functional and structural analysis of the human SLO3 pH- and voltage-gated K^+ channel. *Proc. Natl. Acad. Sci. U.S.A.* **109,** 19274–19279
10. Jiang, Y., Lee, A., Chen, J., Cadene, M., Chait, B. T., and MacKinnon, R. (2002) Crystal structure and mechanism of a calcium-gated potassium channel. *Nature* **417,** 515–522
11. Adelman, J. P., Shen, K. Z., Kavanaugh, M. P., Warren, R. A., Wu, Y. N., Lagrutta, A., Bond, C. T., and North, R. A. (1992) Calcium-activated potassium channels expressed from cloned complementary DNAs. *Neuron* **9,** 209–216
12. Atkinson, N. S., Robertson, G. A., and Ganetzky, B. (1991) A component of calcium-activated potassium channels encoded by the *Drosophila slo* locus. *Science* **253,** 551–555
13. Butler, A., Tsunoda, S., McCobb, D. P., Wei, A., and Salkoff, L. (1993) mSlo, a complex mouse gene encoding "maxi" calcium-activated potassium channels. *Science* **261,** 221–224
14. Schreiber, M., Yuan, A., and Salkoff, L. (1999) Transplantable sites confer calcium sensitivity to BK channels. *Nat. Neurosci.* **2,** 416–421
15. Martínez-López, P., Santi, C. M., Treviño, C. L., Ocampo-Gutiérrez, A. Y., Acevedo, J. J., Alisio, A., Salkoff, L. B., and Darszon, A. (2009) Mouse sperm K^+ currents stimulated by pH and cAMP possibly coded by Slo3 channels. *Biochem. Biophys. Res. Commun.* **381,** 204–209
16. Santi, C. M., Butler, A., Kuhn, J., Wei, A., and Salkoff, L. (2009) Bovine and mouse SLO3 K^+ channels: evolutionary divergence points to an RCK1 region of critical function. *J. Biol. Chem.* **284,** 21589–21598
17. Swanson, W. J., and Vacquier, V. D. (2002) The rapid evolution of reproductive proteins. *Nat. Rev. Genet.* **3,** 137–144
18. Torgerson, D. G., Kulathinal, R. J., and Singh, R. S. (2002) Mammalian sperm proteins are rapidly evolving: evidence of positive selection in functionally diverse genes. *Mol. Biol. Evol.* **19,** 1973–1980
19. Wyckoff, G. J., Wang, W., and Wu, C. I. (2000) Rapid evolution of male reproductive genes in the descent of man. *Nature* **403,** 304–309
20. Podlaha, O., Webb, D. M., Tucker, P. K., and Zhang, J. (2005) Positive selection for indel substitutions in the rodent sperm protein catsper1. *Mol. Biol. Evol.* **22,** 1845–1852
21. Schreiber, M., and Salkoff, L. (1997) A novel calcium-sensing domain in the BK channel. *Biophys. J.* **73,** 1355–1363
22. Xia, X. M., Zeng, X., and Lingle, C. J. (2002) Multiple regulatory sites in large-conductance calcium-activated potassium channels. *Nature* **418,** 880–884
23. Hou, S., Horrigan, F. T., Xu, R., Heinemann, S. H., and Hoshi, T. (2009) Comparative effects of H^+ and Ca^{2+} on large-conductance Ca^{2+}- and voltage-gated Slo1 K^+ channels. *Channels* **3,** 249–258
24. Yusifov, T., Javaherian, A. D., Pantazis, A., Gandhi, C. S., and Olcese, R. (2010) The RCK1 domain of the human BKCa channel transduces Ca^{2+} binding into structural rearrangements. *J. Gen. Physiol.* **136,** 189–202
25. Budelli, G., Geng, Y., Butler, A., Magleby, K. L., and Salkoff, L. (2013) Properties of Slo1 K^+ channels with and without the gating ring. *Proc. Natl. Acad. Sci. U.S.A.* **110,** 16657–16662
26. Yang, C., Zeng, X. H., Zhou, Y., Xia, X. M., and Lingle, C. J. (2011) LRRC52 (leucine-rich-repeat-containing protein 52), a testis-specific auxiliary subunit of the alkalization-activated Slo3 channel. *Proc. Natl. Acad. Sci. U.S.A.* **108,** 19419–19424
27. Sasaki, S., Ishibashi, K., Nagai, T., and Marumo, F. (1992) Regulation mechanisms of intracellular pH of *Xenopus laevis* oocyte. *Biochim. Biophys. Acta* **1137,** 45–51
28. Fraire-Zamora, J. J., and González-Martínez, M. T. (2004) Effect of intracellular pH on depolarization-evoked calcium influx in human sperm. *Am. J. Physiol. Cell Physiol.* **287,** C1688–C1696
29. Hamamah, S., and Gatti, J. L. (1998) Role of the ionic environment and internal pH on sperm activity. *Hum. Reprod.* **13,** Suppl. 4, 20–30
30. Zhang, X., Zeng, X., Xia, X. M., and Lingle, C. J. (2006) pH-regulated Slo3 K^+ channels: properties of unitary currents. *J. Gen. Physiol.* **128,** 301–315
31. Turner, L. M., Chuong, E. B., and Hoekstra, H. E. (2008) Comparative analysis of testis protein evolution in rodents. *Genetics* **179,** 2075–2089
32. Chávez, J. C., de la Vega-Beltrán, J. L., Escoffier, J., Visconti, P. E., Treviño, C. L., Darszon, A., Salkoff, L., and Santi, C. M. (2013) Ion permeabilities in mouse sperm reveal an external trigger for SLO3-dependent hyperpolarization. *PLoS One* **8,** e60578
33. Chávez, J. C., Ferreira, J. J., Butler, A., De La Vega Beltrán, J. L., Treviño, C. L., Darszon, A., Salkoff, L., and Santi, C. M. (2014) SLO3 K^+ channels control calcium entry through CATSPER channels in sperm. *J. Biol. Chem.* **289,** 32266–32275
34. Yuan, P., Leonetti, M. D., Pico, A. R., Hsiung, Y., and MacKinnon, R. (2010) Structure of the human BK channel Ca^{2+}-activation apparatus at 3.0 Å resolution. *Science* **329,** 182–186
35. Xia, X. M., Zhang, X., and Lingle, C. J. (2004) Ligand-dependent activation of Slo family channels is defined by interchangeable cytosolic domains. *J. Neurosci.* **24,** 5585–5591
36. Cross, N. L., and Razy-Faulkner, P. (1997) Control of human sperm intracellular pH by cholesterol and its relationship to the response of the acrosome to progesterone. *Biol. Reprod.* **56,** 1169–1174
37. Gonzalez-Perez, V., Xia, X. M., and Lingle, C. J. (2014) Functional regulation of BK potassium channels by γ1 auxiliary subunits. *Proc. Natl. Acad. Sci. U.S.A.* **111,** 4868–4873
38. McCobb, D. P., Fowler, N. L., Featherstone, T., Lingle, C. J., Saito, M., Krause, J. E., and Salkoff, L. (1995) A human calcium-activated potassium channel gene expressed in vascular smooth muscle. *Am. J. Physiol. Heart Circ. Physiol.* **269,** H767–H777
39. Wei, A., Solaro, C., Lingle, C., and Salkoff, L. (1994) Calcium sensitivity of BK-type KCa channels determined by a separable domain. *Neuron* **13,** 671–681
40. Yuan, A., Dourado, M., Butler, A., Walton, N., Wei, A., and Salkoff, L. (2000) SLO-2, a K^+ channel with an unusual Cl^- dependence. *Nat. Neurosci.* **3,** 771–779